NACA RM E52C11

c 2

RESEARCH MEMORANDUM

DISTRIBUTION OF FISSIONABLE MATERIAL IN THERMAL REACTORS OF SPHERICAL GEOMETRY FOR UNIFORM POWER GENERATION

By Robert R. McCready, Robert B. Spooner and Michael F. Valerino

Lewis Flight Propulsion Laboratory
Cleveland, Ohio

NATIONAL ADVISORY COMMITTEE
FOR AERONAUTICS

WASHINGTON
June 1952
Declassified June 24, 1958

NACA RM E52C11

NATIONAL ADVISORY COMMITTEE FOR AERONAUTICS

RESEARCH MEMORANDUM

DISTRIBUTION OF FISSIONABLE MATERIAL IN THERMAL REACTORS OF SPHERICAL GEOMETRY FOR UNIFORM POWER GENERATION

By Robert R. McCready, Robert B. Spooner
and Michael F. Valerino

SUMMARY

The two-group equations for reflected thermal reactors of spherical geometry are solved for constant power generation over the reactor-core volume. Solution is obtained both analytically and by means of an electrical analogue simulator. Illustrative calculations are made for specified core and reflector compositions and a range of reflector thicknesses to obtain the distributions of fissionable material over the reactor volume required to give uniform power generation. Calculations are also made, for the specific reactors investigated, of the permissible increase in total reactor power output due to uniform power generation, assuming the reactor structural and coolant heat-transfer characteristics to be such that the reactor power is limited by maximum heat-flux rate. The calculations show that for reactors with moderate or thick reflectors substantial increase in reactor power output can be achieved for limiting maximum heat-flux rate within the reactor with only a small additional investment in fissionable material.

For other heat-release limitations in the reactor, for example, maximum fuel-element temperature, the power distribution that leads to maximum total reactor power output will differ from the uniform power case treated herein. However, comparable increases in permissible power output and fissionable-material investment are to be expected. The results presented herein therefore illustrate the advantage of distributing the fissionable material within the reactor in such a manner that each reactor volume element is operating at, or very near to, the particular limiting heat-release condition existing for the given reactor.

Both the analytical and simulator solutions adapt readily to specified radial power distributions other than uniform.

INTRODUCTION

The power that a reactor delivers can be increased by (1) a more effective heat-transfer system and (2) nonuniform distribution of the

uranium fuel to increase the power generated in regions where it is low, so that each part of the reactor core operates with maximum effectiveness. In many reactors the disturbance of the power distribution produced by the control-rod system makes step (2) of little use. As a consequence of the normal variation in power density over the core and its further distortion by the insertion of control rods, the over-all heat release, as averaged over the reactor volume, may be of the order of a one half or one third of the maximum heat release permissible on the basis of such practical considerations as high-temperature strength of the metal surfaces across which the fission energy is transferred to the coolant, thermal stresses induced in the heat-transmitting surface, and so forth.

Numerous schemes are being actively considered for eliminating the use of the conventional control rods. For example, in reference 1, a supercritical water reactor is proposed wherein the reactor control is to be accomplished by variation in water density (and hence in neutron-moderating properties of the water) accompanying pressure and temperature change. Consideration is also being given to the use of a strong neutron absorber dissolved in the coolant with provisions for continuously varying the absorber concentration so as to control the relatively slow reactivity changes accompanying xenon build-up and fuel burn-up. The short-period fast-reactivity changes would then be controlled by only a small group of conventional control rods.

For these systems, it is of interest to study the gains to be realized by distribution of the fissionable material nonuniformly over the reactor volume. In order to evaluate the feasibility of this scheme, knowledge is required of the change in fuel requirement accompanying the permissible gain in reactor power output.

An analytical method of solution, which was derived at the NACA Lewis laboratory, is presented herein of the two-group equations for reflected thermal reactors of spherical geometry for the special case of uniform power generation over the reactor volume. Calculations are made, for a series of reactors of specified core and reflector compositions and various reflector thicknesses, to illustrate the magnitude of the extra fuel investment due to uniform reactor-power generation. Also, the permissible increase in reactor power output due to uniform power generation is calculated assuming the reactor structure and coolant-flow conditions to be such that the reactor power is limited by maximum heat-flux rate.

In addition to the analytical method of solution, solutions were obtained by means of an electrical analogue simulator. With the analogue simulator, the condition of uniform power generation was approached in steps so that results were also obtained for power-generation patterns successively approaching the uniform pattern. The results thereby obtained are useful in establishing to what degree the condition of uniform power generation is desirable for limiting heat-flux rate conditions.

SYMBOLS

The following symbols are used in this report:

D	d/dr
$g(r)$	$N(r)/N_s$
$H(r)$	power density at radius r from center of reactor
H_{max}	maximum power density in reactor
H_{av}	average power density over volume of reactor core
I	fissionable material investment for variable concentration case
I_s	fissionable material investment for standard case of uniform concentration
i	current forced into simulator network section
$k_{th} = \frac{\nu \Sigma_{F,th}}{\Sigma_{a,th}}$	thermal multiplication constant
L_f	fast diffusion length
L_{th}	thermal diffusion length
$N(r)$	concentration of fissionable material at radius r from center of spherical reactor
$\overline{N} = \frac{1}{V}\int N(r)dV$	average value of fissionable material concentration over reactor core volume
N_s	concentration of fissionable material for standard case of uniform fissionable material distribution
p_{th}	resonance escape probability
R_a	network resistor simulating absorption of neutrons by materials other than uranium. For fast neutron group, this includes slowing down of neutrons out of group.

R_u	network resistor simulating absorption of neutrons by uranium
$R\phi$	network resistor simulating neutron diffusion properties of reactor region
r	space coordinate
r_c	critical radius of reactor core
t	reflector thickness
V	reactor core volume
U,X,Y	matrices
α	variation parameter
∇^2	$\frac{d^2}{dr^2} + \frac{2}{r}\frac{d}{dr}$
λ_{tr}	transport mean free path
υ	number of neutrons produced per fission
Σ_a	macroscopic absorption cross section (when applied to fast group, includes neutron loss due to slowing out of the group)
$\Sigma_{a,th}^{M}$	macroscopic absorption cross section for thermal neutrons of all materials in reactor core excepting uranium
$\Sigma_{a,f}^{M}$	value of $\Sigma_{a,f}$ excluding absorption by uranium
Σ_F	macroscopic fission cross section
σ_a^u	microscopic absorption cross section for uranium
σ_F^u	microscopic fission cross section for uranium
θ	$r\phi_f$

ϕ_f	fast neutron flux
ϕ_{th}	thermal neutron flux
ψ	$r\phi_{th}$

Subscripts:

f,th	fast and thermal parameters, respectively

Superscripts:

Primed superscript indicates reflector parameter.

No superscript indicates a core parameter.

Arbitrary constants:

A, B, P, Q

Parameter groupings:

$$a = \frac{3\Sigma_{a,f}}{\lambda_{tr,f}} = \frac{1}{L_f^2}$$

$$b = \frac{3k_{th}\Sigma_{a,th}}{\lambda_{tr,f}}$$

$$C_1 = \frac{3\Sigma_{F,th}\phi_{th}\nu}{\lambda_{tr,f}}$$

$$C_2 = \frac{\lambda_{tr,f}}{\lambda_{tr,th}} \frac{\sigma_a^u}{\nu\sigma_F^u} C_1$$

$$c = \frac{3\Sigma_{a,th}}{\lambda_{tr,th}} = \frac{1}{L_{th}^2}$$

$$\bar{c} = \frac{3\sum_{a,th}^{M}}{\lambda_{tr,th}}$$

$$d = \frac{\Sigma_{tr,f}}{\lambda_{tr,th}} p_{th} \frac{1}{L_f^2}$$

$$f = \frac{1}{L'^2_f}$$

$$g = \frac{1}{L'^2_{th}}$$

$$m = p'_{th} \frac{\lambda'_{tr,f}}{\lambda'_{tr,th}} \frac{1}{L'^2_f}$$

ANALYSIS

The system of two-group equations for a critical reflected thermal reactor are:

$$\frac{\lambda_{tr,f}}{3} \nabla^2 \phi_f - \Sigma_{a,f} \phi_f + k_{th} \Sigma_{a,th} \phi_{th} = 0 \tag{1}$$

$$\frac{\lambda_{tr,th}}{3} \nabla^2 \phi_{th} - \Sigma_{a,th} \phi_{th} + p_{th} \Sigma_{a,f} \phi_f = 0 \tag{2}$$

$$\frac{\lambda'_{tr,f}}{3} \nabla^2 \phi'_f - \Sigma'_{a,f} \phi'_f = 0 \tag{3}$$

$$\frac{\lambda'_{tr,th}}{3} \nabla^2 \phi'_{th} - \Sigma'_{a,th} \phi'_{th} + p'_{th} \Sigma'_{a,f} \phi'_f = 0 \tag{4}$$

The solutions of these equations are subject to the four boundary conditions:

$$\phi_f(0) < \infty \tag{5}$$

$$\phi_{th}(0) < \infty \tag{6}$$

$$\phi'_f(r_c+t) = 0 \tag{7}$$

$$\phi'_{th}(r_c+t) = 0 \tag{8}$$

and to the four continuity conditions:

$$\phi_f(r_c) = \phi'_f(r_c) \tag{9}$$

$$\phi_{th}(r_c) = \phi'_{th}(r_c) \tag{10}$$

$$\lambda_{tr,f} D \phi_f(r_c) = \lambda'_{tr,f} D \phi_f'(r_c) \tag{11}$$

$$\lambda_{tr,th} D \phi_{th}(r_c) = \lambda'_{tr,th} D \phi'_{th}(r_c) \tag{12}$$

The problem is to determine, for assignable core and reflector sizes and compositions, the amount and the distribution of fissionable material over the reactor volume required to satisfy both criticality and the condition of uniform power generation over the reactor core volume.

In a thermal reactor (that is, wherein the fast-neutron absorption by the fissionable material is negligibly small compared with the thermal-neutron absorption), the parameters $\lambda_{tr,f}$, $\Sigma_{a,f}$, p_{th}, and $\lambda_{tr,th}$ in equations (1) and (2) are fairly insensitive to large variations in fissionable-material concentration. Hence, these parameters are assumed as constant in the analysis; the degree of validity of this assumption for any specific problem can be evaluated from the fissionable material concentrations calculated for the specific problem.

Two different methods of approach are used in the analysis, one analytical and the other by means of an electrical analogue simulator designed for solution of multigroup equations (reference 2). In both methods, the analysis is based on the assumption of spherical geometry.

Analytical solution. - For spherical geometry, the two-group diffusion equations in the reactor core (equations (1) and (2)) can be written in the form

$$D^2 \theta - a\theta + b\psi = 0 \tag{13}$$

$$D^2 \psi - c\psi + d\theta = 0 \tag{14}$$

$$\theta = r\phi_f \tag{15}$$

$$\psi = r\phi_{th} \tag{16}$$

For uniform heat generation in a thermal reactor, the relation

$$\Sigma_{F,th}\,\phi_{th} = \text{constant} \tag{17}$$

must hold throughout the reactor core. Equations (13) and (14), with the condition stipulated in equation (17), reduce to

$$D^2\theta - a\theta + C_1 r = 0 \tag{18}$$

and

$$D^2\psi - \bar{c}\psi - C_2 r + d\theta = 0 \tag{19}$$

in which

$$C_1 = \frac{3\Sigma_{F,th}\phi_{th}\nu}{\lambda_{tr,f}} \tag{20}$$

$$C_2 = \frac{\lambda_{tr,f}}{\lambda_{tr,th}} \frac{\sigma_a u}{\nu\sigma_F u} C_1 \tag{21}$$

$$\bar{c} = \frac{3\sum^{M}_{a,th}}{\lambda_{tr,th}} \tag{22}$$

In the solution of equations (18) and (19), the fast parameters and thermal scattering parameters are assumed unaffected by variation in concentration of fissionable material over the reactor core. This assumption is valid for the thermal reactors considered herein provided that the attainment of uniform power generation does not necessitate highly enriched concentration of fissionable material in any portion of the reactor core volume.

The solutions of equations (18) and (19) are

$$\theta = A \sinh\sqrt{a}r + \frac{C_1}{a} r \tag{23}$$

$$\psi = \frac{d}{c-a} A \sinh\sqrt{a}r + B \sinh\sqrt{c}r + \frac{1}{c}\left(\frac{dC_1}{a} - C_2\right)r \tag{24}$$

The hyperbolic cosines, which constitute a portion of the complementary function, have been eliminated by application of boundary conditions (5) and (6).

The reflector equations (3) and (4) are unaltered in form by variation in fissionable material concentration over the reactor core. For spherical symmetry, equations (3) and (4) become

$$D^2\theta - f\theta = 0 \tag{25}$$

$$D^2\psi - g\psi + m\theta = 0 \tag{26}$$

The solutions to equations (25) and (26) that vanish at the outer reflector boundary are

$$\theta = P \sinh\sqrt{f}\,(r_c+t-r) \tag{27}$$

$$\psi = \frac{m}{g-f} P \sinh\sqrt{f}\,(r_c+t-r) + Q \sinh\sqrt{g}\,(r_c+t-r) \tag{28}$$

The fluxes resulting from equations (23), (24), (27), and (28) are

$$\phi_f = \frac{A}{r} \sinh\sqrt{a}r + \frac{C_1}{a} \tag{29}$$

$$\phi_{th} = \frac{d}{c-a}\frac{A}{r} \sinh\sqrt{a}r + \frac{B}{r} \sinh\sqrt{c}r + \frac{1}{c}\left(\frac{dC_1}{a} - C_2\right) \tag{30}$$

$$\phi'_f = \frac{P}{r} \sinh\sqrt{f}\,(r_c+t-r) \tag{31}$$

$$\phi'_{th} = \frac{m}{g-f}\frac{P}{r} \sinh\sqrt{f}\,(r_c+t-r) + \frac{Q}{r} \sinh\sqrt{g}\,(r_c+t-r) \tag{32}$$

The boundary conditions of equations (7) and (8) have been utilized in the choice of form for these solutions. The continuity conditions (9) to (12) give rise to four simultaneous equations for A, B, P, and Q. A more detailed account of these equations and their implications toward criticality is indicated in appendix A.

The arbitrary nature of the actual power level implied by equation (17) enables C_1 to be taken as any positive constant in equations (29) and (30).

Equation (20) with $C_1 = 1$ can therefore be written as

$$\frac{\lambda_{tr,f}}{3\nu\phi_{th}(r)} = \Sigma_{F,th}(r) \tag{33}$$

from which the value of $\Sigma_{F,th}(r)$ corresponding to the thermal flux $\phi_{th}(r)$ is determined.

In order to compare the fissionable material investment for variable concentration with that for uniform concentration, N_s is defined as the uniform concentration required in a reactor of the same size and composition (except for amount of fissionable material) as that for the variable concentration case. It is assumed that N_s has been determined by the usual procedures for uniform distribution of fissionable material.

Let

$$g(r) = \frac{N(r)}{N_s} = \frac{\Sigma_{F,th}(r)}{\Sigma_{F,th_s}} \tag{34}$$

The investment for variable concentration is

$$I = \bar{N}V \tag{35}$$

and for the case of uniform concentration is

$$I_s = N_s V \tag{36}$$

where $\bar{N}$ is the average concentration over the reactor volume as given by

$$\bar{N} = \frac{1}{V}\int_{core} N(r)\, dV \tag{37}$$

Hence,

$$\frac{I}{I_s} = \frac{\bar{N}}{N_s} \tag{38}$$

which, for spherical geometry, gives

$$\frac{I}{I_s} = \frac{4\pi \int_0^{r_c} r^2 g(r)\, dr}{4/3\ \pi r_c^3} = \frac{3}{r_c^3} \int_0^{r_c} r^2 g(r)\, dr \qquad (39)$$

In the cases investigated, the integral of equation (39) was evaluated by numerical integration using Simpson's three-point rule.

Although the foregoing procedure treats only uniform heat generation, a wide variety of other radial distributions can be handled. A specific example of another power distribution and the approach to more general ones is indicated in appendix B.

Electrical analogue simulator solution. - The distribution of uranium necessary for a prescribed reactor power distribution can also be determined with the aid of an electrical analogue network. A brief description of the NACA nuclear reactor simulator and an outline of the procedure followed in obtaining the solutions for this analysis are presented with the aid of figure 1. This simplified schematic diagram identifies the various components of the simulator network with the corresponding volume elements of the reactor segment under investigation. Further details about the NACA nuclear reactor simulator appear in reference 2.

The two-group reactor solutions obtained with the simulator required two networks similar to that in figure 1; one for the fast group of neutrons and one for the thermal group. The segment of a spherical reactor bounded by some solid angle and divided radially into volume elements is shown in figure 1. Each volume element appears directly above its associated network section. The resistors in each of these network sections are determined by their required relations to the various neutron-diffusion, absorption, and slowing-down properties of the materials making up the reactor volume element. If the currents i_1, i_2, . . . introduced into each network section are made proportional to the number of neutrons in the corresponding reactor volume element that are entering the desired neutron energy range (neutron group) per unit time, the potentials measured on the network junction points become proportional to the neutron fluxes in the simulated volume elements. In addition, the current through any resistor in the network becomes proportional to the number of neutrons of that energy group undergoing the process simulated by the resistor. A detailed listing of the simulator components, the nuclear processes simulated by the currents through the components, and the primary nuclear variables on which the components are dependent appears in table I. Components are described for both fast and thermal networks.

The procedure followed herein is based on the requirement that the critical reactor must supply and maintain a specified distribution of fission neutrons. This requirement fixes the currents i entering the fast network, and the specified reactor composition determines the values used for the network resistors (reference 2). By means of the simulator, a typical "generation of neutrons" is followed through its life cycle and the R_u resistors are adjusted to produce an identical new generation of neutrons. These adjustments relate to changes in the concentration of uranium in each reactor volume element. The following steps outline the solution process.

Fast group:

(1) The resistors in the fast network are adjusted to the prescribed values. The R_u resistor is removed because fissions due to fast neutrons are negligible in the cases discussed herein.

(2) The currents i are adjusted in proportion to the fission neutron distribution assumed to form the generation. This distribution is proportional to that for the prescribed power generation because both are dependent on the rate of fissions at any point.

(3) The voltage at each junction point of the network gives a quantity proportional to the fast neutron flux.

(4) The currents through the resistors R_a are measured and multiplied by the resonance escape probability. These resultant values are proportional to the neutrons slowing down out of the fast group.

Thermal group:

(5) The resistors are adjusted to the proper values for the thermal network.

(6) The currents i are adjusted to be proportional to the previously measured number of neutrons slowing down from the fast group. For criticality, the currents through the R_u resistors, multiplied by the proper multiplication constant, should be equal to the prescribed currents i forced into the fast network (that is, to the currents representing the specified fission neutron distribution). Further details about determining the multiplication constant appear in reference 2.

(7) If only the sum of the currents through the R_u resistors multiplied by the multiplication constant equals the sum of the inputs to the fast network, the reactor can be considered to be critical, but not adjusted for proper power generation. Each R_u resistor is then adjusted by an amount proportional to the deviation in the measured current through it from the required current. The amount of change must also be such as to maintain criticality in the reactor.

The intermediate solution obtained by the foregoing steps approximates the steady-state solution for the uranium distribution on which it depends. The usefulness of this solution is considered following step (11).

(8) After this adjustment of R_u resistors, the new currents through the R_u resistors will again deviate from the desired solution, but will give a closer approximation and indicate further adjustments repeated as in step (7).

(9) The sequence of solutions obtained by repetition of steps (7) and (8) converges on the desired reactor solution and also provides a set of intermediate solutions that prove useful if, in each solution, the distribution of currents through the R_u resistors indicates a new generation of neutrons approximately like the original distribution of fission neutrons.

(10) If only the final solution is desired, the R_u resistors can be varied individually until the proper current is indicated through each. This one-step method is especially useful for reactors with thin reflectors for which the intermediate solutions would be of little value because they lead to generations of neutrons much different from the original distribution of fission neutrons.

(11) The fractional decrease in each R_u resistor required in the last four steps is the same as the fractional increase in uranium in the corresponding reactor volume element. The current through each resistor is proportional to the number of fissions taking place and, therefore, to the power generated in the associated volume element.

A set of power generation curves and the required uranium distributions are produced almost directly by the preceding steps. The procedure gives a sequence of solutions that approach the initially specified power distribution. These approximate intermediate solutions are useful for estimating the power distributions attainable with smaller uranium investments than those required for uniform power generation and indicate whether the initially specified power distribution is the most advantageous one to obtain high reactor performance from the standpoint of fissionable material investment.

The foregoing procedure demonstrates the adaptability of the nuclear reactor simulator to the rapid solution of problems requiring the redistribution of fissionable material in a reactor. The simulator permits quick and convenient simulation of the variation of properties of the reactor materials and, from the measured quantities, a direct interpretation of the effect of these variations on the uranium distribution and total investment and the power generation in the reactor.

CONDITIONS FOR ILLUSTRATIVE CALCULATIONS

The core and reflector parameters chosen for the illustrative calculations correspond to those for certain water-moderated and cooled thermal reactors utilizing a water reflector. The values of these parameters are

$$\sum_{a,th}^{M} = 0.0119 \qquad L_f^2 = 64$$

$$\lambda_{tr,f} = 3.78 \qquad L_{th}^2 = 3.64$$

$$\lambda_{tr,th} = 0.79 \qquad L'^2_f = 33$$

$$\lambda'_{tr,f} = 3.43 \qquad L'^2_{th} = 8.3$$

$$\lambda'_{tr,th} = 0.43 \qquad p_{th} = 0.95$$

$$p'_{th} = 0.98$$

Reactor sizes investigated are:

Reactor	Core radius (cm)	Reflector thickness (cm)
I	24	16
II	26	8
III	30	4

The fissionable material investments required to maintain criticality for the case of uniform fissionable material distribution are 2.11, 2.69, and 3.74 kilograms for reactors I, II, and III, respectively.

EXAMPLE OF COMPARISON OF REACTOR POWER

The maximum power limitation of a reactor varies with each design depending on such factors as materials in the reactor and their strength characteristics, arrangement and design of heat-transfer surfaces, coolant, coolant flow path, and so forth. Hence, without consideration of these detailed design factors, it is impossible to assign any specific criterion for comparing limiting power outputs of reactors.

For illustrative purposes, consider a reactor with the following heat-transfer and strength characteristics which result in maximum heat-flux rate as the heat-release limitation for the reactor.

(1) The coolant has a high heat-transfer coefficient and undergoes only a small temperature change in the reactor core. The walls of the entire flow passage then operate at approximately the same inside temperature.

(2) Heat is conducted to the coolant through material having relatively low thermal conductivity and low resistance to thermal stress because of the resulting temperature gradient through the material. For this specific example, uniform power generation at the stress-limiting heat-flux rate will result in the maximum power that can be generated within the reactor-core volume.

Based on the criterion of limiting heat-flux rate, the power outputs of reactors I, II, and III (listed in foregoing section) with uniform fissionable material concentration are compared with the power outputs of these same reactors wherein the fissionable material is redistributed in a manner to attain uniform power generation.

For other criterions, for example, constant coolant-passage-wall temperature, the power generation leading to maximum total-power output of the reactor will vary with the coolant conditions and flow paths.

RESULTS AND DISCUSSION

Analytical Solution

The results of the analytical solutions for the three cases listed in the foregoing section are presented in figures 2 to 4.

Figures 2(a), 3(a), and 4(a) indicate the normalized power generation curves for the three reactors investigated. The average-to-maximum power ratio H_{av}/H_{max} for the case of uniform fissionable material concentration are 0.76, 0.73 and 0.53 for reactors I, II, and III, respectively, compared with 1.00 for the case of uniform power production. Hence, uniform power generation in reactors I, II, and III results in 32, 37, and 89 percent increases, respectively, in total permissible power output for a stress limiting heat-flux rate. The minimums of the power generation curves for reactors I, II, and III are about 33, 37.5, and 68 percent below the maximums, indicating the sharp departures from uniformity in heat generation that are typical of reactors having uniform concentration.

The distribution of fissionable material necessary to maintain uniform heat generation for the indicated critical radii and reflector thicknesses is presented in figures 2(b), 3(b), and 4(b). The aid given by the reflector in preventing serious increments in investment manifests

itself in the relatively low maximums and moderate interface values attained in the concentration curve for the first two cases. A much more extreme maximum and interface value prevail in the third case where the reflector thickness is insufficient to supply adequate feedback of thermal neutrons. The relative increases in investment in the three cases are 9, 15, and 197 percent, respectively, indicating that moderate and thick reflectors do not seriously alter investment requirements necessary to maintain uniform heat generation, but that thin reflectors cause the investment to suffer a decisive increase. Because of the large local concentration of fissionable material required in the vicinity of the reflector for reactor III, the assumption of invariance of fast parameters made in the analysis is not strictly valid for this case, although the general shape of the curves obtained is probably representative.

The thermal fluxes of figures 5 to 7 follow the same general shape of fluxes established in reactors of uniform uranium distribution. The decreased slope at the interface, which accompanies decreased reflector thickness again provides the anticipated evidence of reflector effectiveness.

Simulator Solution

The power generation and corresponding fissionable material distributions found with the aid of the nuclear reactor simulator for the three assemblies investigated are presented in figures 8 to 10.

For reactors I and II, these distributions are shown in figures 8 and 9, respectively. The successive changes in power distribution that were determined on the simulator give a progression of curves approaching the desired uniform distribution. The minimum local value of power generation relative to the maximum value in reactor I was raised from 0.67 to 1.00 by only a 6 percent increase in uranium distributed as shown by curves A (figs. 8(a) and 8(b)). This reactor had an average power generation only 0.752 of the maximum value. Similar changes made in reactor II, where the original minimum power generation value was only 0.62 of the maximum rate, required only 10 percent increase in uranium distributed according to curves A (figs. 9(a) and 9(b)). The average power generation in the reactor was also increased from 0.725 of the maximum value to a uniform generation at maximum value.

Three different degrees of improvement in power generation were considered for reactor III as shown in figure 10 together with the power distribution for uniform fissionable material concentration. In two of the power distributions, the power generation decreased linearly with reactor core radius to 0.9 and 0.8 of the maximum power generation. The third corresponded to uniform power generation. The improved

power-generation distributions were obtained at the price of a considerable additional investment in uranium as indicated in figure 10(b). For uniform power generation in the thinly reflected reactor III, it was necessary to increase the uranium investment by 225 percent. This material, distributed according to curve A in figure 10(b), raised the average power generation in the reactor from 0.529 of the maximum value to uniform maximum power generation.

The thermal neutron fluxes in reactors I, II, and III corresponding to uniform power generation are shown in figures 11, 12, and 13, respectively, for comparison with those found by numerical calculations. In addition, the fluxes for the intermediate power distributions are included for each reactor.

Figures 8(b), 9(b), and 10(b) show approximately the same uranium distribution curves as the corresponding results of numerical calculations on figures 2(b), 3(b), and 4(b). In all cases, the deviations between results are greatest in regions where the spatial variation in uranium concentration is greatest. In these regions, the size of the radial interval assigned to a simulator network section led to a less accurate approximation of the nuclear variables. This limitation of accuracy is shown further by the curves of reactor flux in figures 11 to 13, as compared with the numerically calculated fluxes shown in figures 5 to 7. The maximum percent deviation in flux values amounts to approximately 10 percent and occurs at the core-reflector boundary in reactor III. The deviations in values also affect the total uranium investment as shown on the following table:

Reactor	I/I_s	
	Calculated	Simulator
I	1.09	1.06
II	1.15	1.10
III	2.97	3.25

The extreme variation in uranium concentration in reactor III again led to the maximum deviation in uranium investment values.

The general agreement between nuclear variables determined with the simulator and by numerical calculations together with the provision for decreasing the radial interval for a network section on the simulator indicates that the simulator procedure can be relied on to closely approximate the results of numerical calculations. The simulator can therefore be applied with confidence for conditions difficult to treat analytically.

SUMMARY OF RESULTS

The two-group equations for reflected thermal reactors of spherical geometry are solved for the case of constant power generation over the reactor core volume. For illustrative purposes, the results of this analysis were used to calculate the increase in reactor power output permissible for a limiting heat-flux rate and the increase in fissionable material required when the fissionable material is distributed in the manner to attain uniform power generation. The calculations show that:

1. For cases I and II which are well moderated thermal reactors with a thick and medium size reflectors, 32 and 37 percent increases in power output were obtained, respectively, at the expense of 9 and 15 percent increases in fissionable material investment.

2. In reactor III, which was likewise a thermal reactor but with a thin reflector, a 89 percent increase in power output was obtained for a 197 percent increase in investment.

Both methods of solution apply to much more general prescribed radial power distributions.

Lewis Flight Propulsion Laboratory
National Advisory Committee for Aeronautics
Cleveland, Ohio, January 11, 1952

APPENDIX A

CRITICALITY DETERMINANT AND EXISTENCE OF MINIMUM CRITICAL RADIUS

For spherical assemblies, the relations of equations (9), (10), (11), and (12) may be expressed by the matrix equation

$$\underset{\downarrow}{UX} = Y \tag{A1}$$

with U, X, and Y, the following 4×4, 4×1, and 4×1 matrices, respectively.

$$U = \begin{bmatrix} \frac{\sinh\sqrt{a}\, r_c}{r_c} & 0 & -\frac{\sinh\sqrt{f}t}{r_c} & 0 \\ \frac{d}{c-a}\frac{\sinh\sqrt{a}\, r_c}{r_c} & \frac{\sinh\sqrt{c}\, r_c}{r_c} & \frac{-m}{g-f}\frac{\sinh\sqrt{f}t}{r_c} & -\frac{\sinh\sqrt{g}t}{r_c} \\ \lambda_{tr,f}\left[\frac{\sqrt{a}\cosh\sqrt{a}\, r_c}{r_c} - \frac{\sinh\sqrt{a}\, r_c}{r_c^2}\right] & 0 & \lambda'_{tr,f}\left[\frac{\sqrt{f}\cosh\sqrt{f}t}{r_c} + \frac{\sinh\sqrt{f}t}{r_c^2}\right] & 0 \\ \frac{d\lambda_{tr,th}}{c-a}\left[\frac{\sqrt{a}\cosh\sqrt{a}\, r_c}{r_c} - \frac{\sinh\sqrt{a}\, r_c}{r_c^2}\right] & \lambda_{tr,th}\left[\frac{\sqrt{c}\cosh\sqrt{c}\, r_c}{r_c} - \frac{\sinh\sqrt{c}\, r_c}{r_c^2}\right] & \frac{m\lambda'_{tr,th}}{g-f}\left[\frac{\sqrt{f}\cosh\sqrt{f}t}{r_c} + \frac{\sinh\sqrt{f}t}{r_c^2}\right] & \lambda'_{tr,th}\left[\frac{\sqrt{g}\cosh\sqrt{g}t}{r_c} + \frac{\sinh\sqrt{g}t}{r_c^2}\right] \end{bmatrix} \tag{A2}$$

$$X = \begin{bmatrix} A \\ B \\ P \\ Q \end{bmatrix} \tag{A3}$$

$$Y = \begin{bmatrix} \frac{C_1}{a} \\ \frac{1}{c}\left(\frac{dC_1}{a} - C_2\right) \\ 0 \\ 0 \end{bmatrix} \tag{A4}$$

The generally nonsingular character of the matrix U of equation (A2) indicates that a solution

$$X = U^{-1}Y \tag{A5}$$

exists for all but possibly a set of isolated values of r_c. The values of A, B, P, and Q resulting from the solution of (A1) determine the fluxes quantitatively.

Equation (33) implies that the required concentration for criticality is inversely proportional to $\phi_{th}(r)$ as obtained by the foregoing procedure. Those values of r_c which give $\phi_{th} \leq 0$ for some $r < r_c$ are not admissible.

For example, in reactor III it was found that, for $r_c = 26.75$ centimeters, $\phi_{th} = 0$ was attained at $r = 24.74$ centimeters (ϕ_f was non-negative throughout the reactor); this implies infinite concentration at this radius. For $r_c < 26.75$ centimeters, ϕ_{th} actually attained negative values at portions of the region $0 < r < r_c$. It is evident that $r_c = 26.75$ centimeters defines the mathematical minimum critical radius for this case. Since a zero thermal flux implies an infinite concentration of fissionable material, the physical lower bound on r_c is somewhat greater than this mathematical bound.

APPENDIX B

SOLUTIONS FOR OTHER RADIAL POWER DISTRIBUTIONS

The physical situation of altering the required heat generation corresponds to the establishment of a new particular integral in the solution of the two-group equations. For example, if a linear variation in heat generation decreasing from the center is required, the core diffusion equations (for a sphere) become

$$D^2\theta - a\theta + C_1 r\,(1-\alpha r) = 0,\quad r \geq 0 \tag{B1}$$

$$D^2\psi - \bar{c}\psi - C_2 r\,(1-\alpha r) + d\theta = 0,\quad r \geq 0 \tag{B2}$$

which have the following suitable solutions:

$$\phi_f = \frac{A \sinh\sqrt{a}r}{r} + \frac{C_1}{a}\left\{1 - \left[\frac{2\alpha}{ar}\,(1 - \cosh\sqrt{a}r) + \alpha r\right]\right\} \tag{B3}$$

$$\phi_{th} = \frac{B \sinh\sqrt{\bar{c}}r}{r} + \frac{d}{\bar{c}-a}\,\frac{A \sinh\sqrt{a}r}{r} + \frac{1}{\bar{c}}\left(\frac{C_1}{a} - C_2\right) +$$

$$\frac{2d\alpha\, C_1}{a^2(\bar{c}-a)}\,\frac{\cosh\sqrt{a}r - 1}{r} + \frac{2}{\bar{c}}\left[\frac{C_2\alpha}{\bar{c}} + \frac{d\alpha\, C_1}{\bar{c}(\bar{c}-a)}\right]\frac{1 + \cosh\sqrt{\bar{c}}r}{r} +$$

$$\frac{1}{\bar{c}}\left(C_2\alpha - \frac{d\alpha\, C_1}{a}\right)r \tag{B4}$$

All variations in $\phi_{th}\,\Sigma_f$ for which a particular integral exists yield themselves to solution by this method. In particular, the large variety of variations that can be represented by, or approximated by polynomials or simple exponentials have easily found particular integrals. If the particular integral is difficult to find, or cumbersome to use explicitly, it can be found numerically and this solution added to the complementary function to obtain the complete integral.

REFERENCES

1. Anon: Application of a Water Cooled and Moderated Reactor to Aircraft Propulsion. Wash-24, August 18, 1950.

2. Spooner, Robert B.: Comparison of Two Group and Multigroup Reactor Solutions for Some Reflected Intermediate Assemblies. NACA RM E52D04, (to be published).

TABLE I - NUCLEAR REACTOR SIMULATOR COMPONENTS

Simulator component	Process simulated by current through component	Relation to primary nuclear variable
	Fast group	
R_{ϕ}	Net number of neutrons/sec diffusing between volume elements	R_{ϕ} inversely proportional to $\lambda_{tr,f}$
R_a	Number of neutrons/sec slowing down out of fast group and being absorbed in materials other than uranium	R_a inversely proportional to $\sum_{a,f}^{m}$
R_u	Number of neutrons/sec absorbed in uranium (if any considered)	R_u inversely proportional to number of U atoms present
i	Number of neutrons/sec born in fission processes by previous neutron generation	i proportional to number of neutrons/sec produced by the specified distribution of fissions in U^{235}
	Thermal group	
R_{ϕ}	Net number of neutrons/sec diffusing between volume elements	R_{ϕ} inversely proportional to $\lambda_{tr,th}$
R_a	Number of neutrons/sec absorbed in material other than uranium	R_a inversely proportional to $\sum_{a,th}^{m}$
R_u	Number of neutrons/sec absorbed in uranium	R_u inversely proportional to number of U atoms present
i	Number of neutrons/sec slowing down into thermal group	i proportional to number of neutrons/sec slowing out of fast group

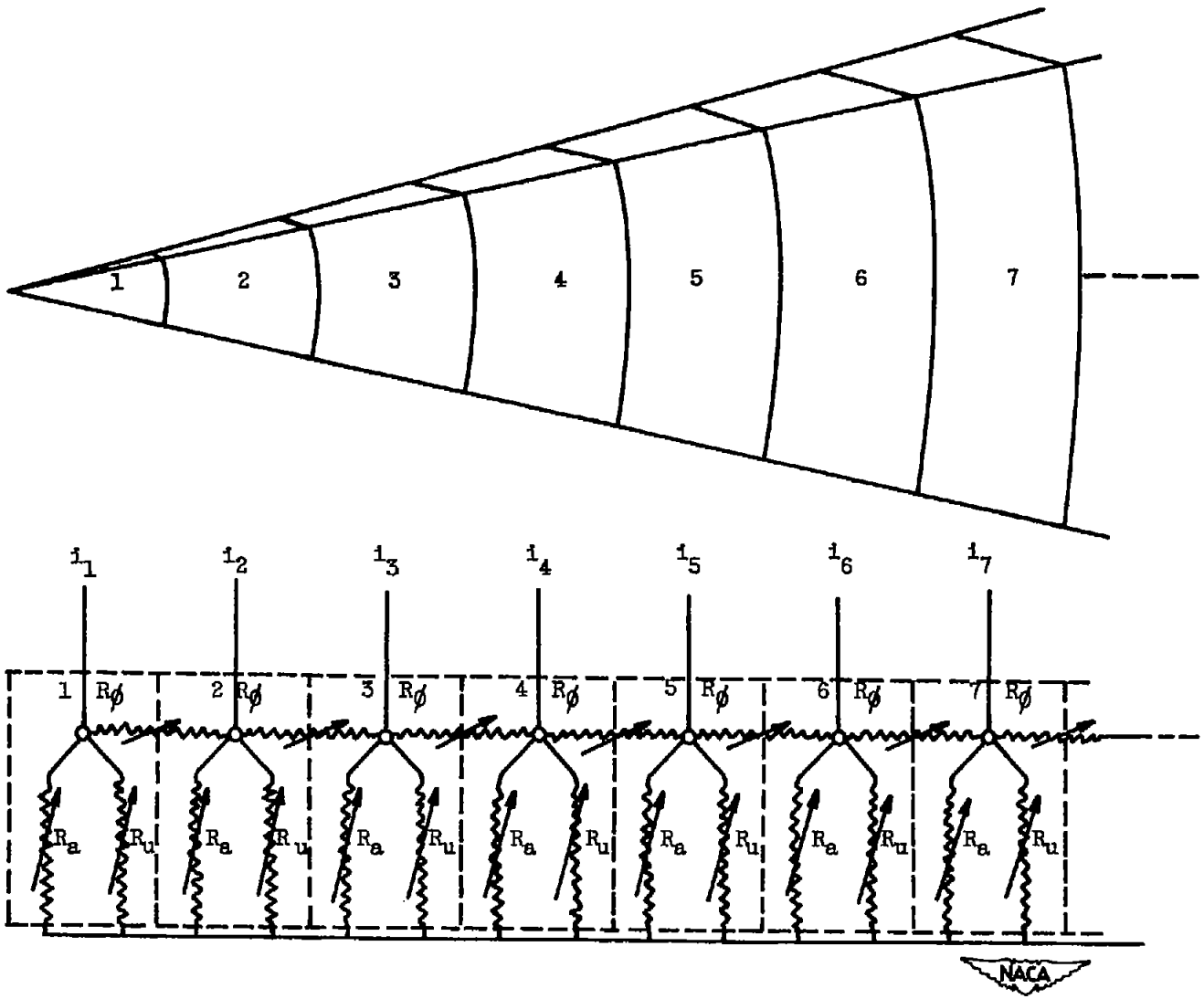

Figure 1. - Reactor segment and corresponding simulator network for one neutron group.

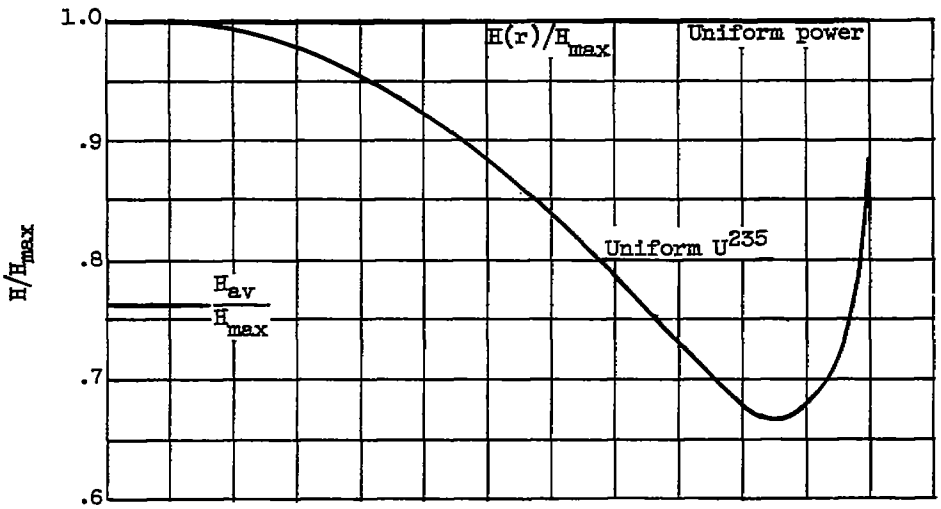

(a) Power generation distribution

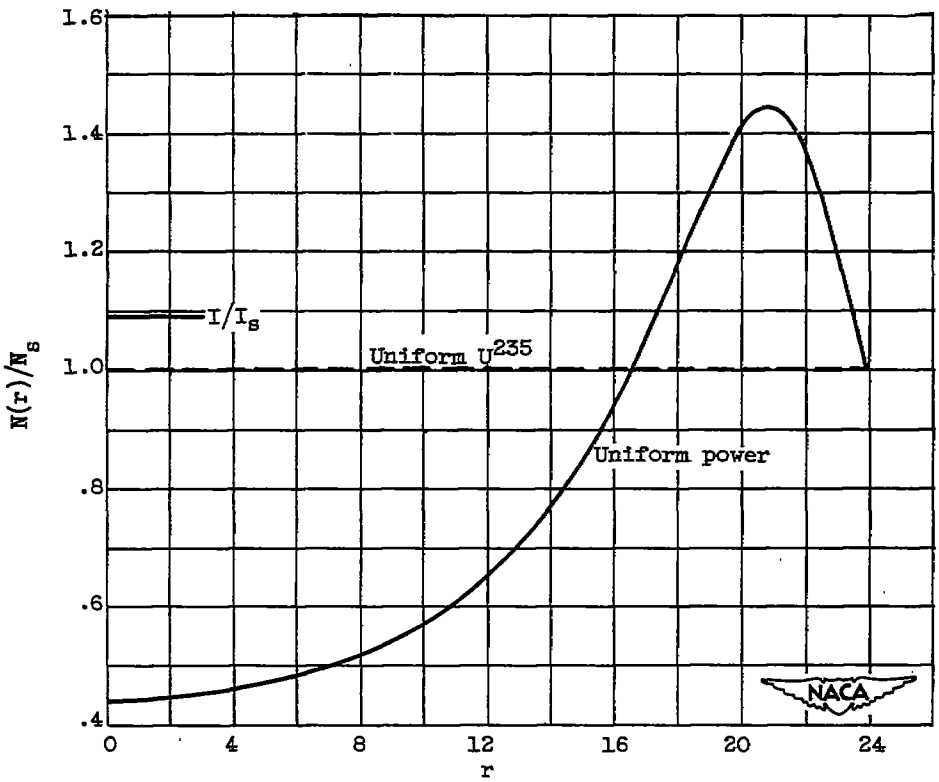

(b) Fissionable material distribution.

Figure 2. - Comparison of power generation and corresponding fissionable material distributions for reactor I, analytical solution. (Relative level of power curves based on a specified limiting heat-flux rate for reactor.)

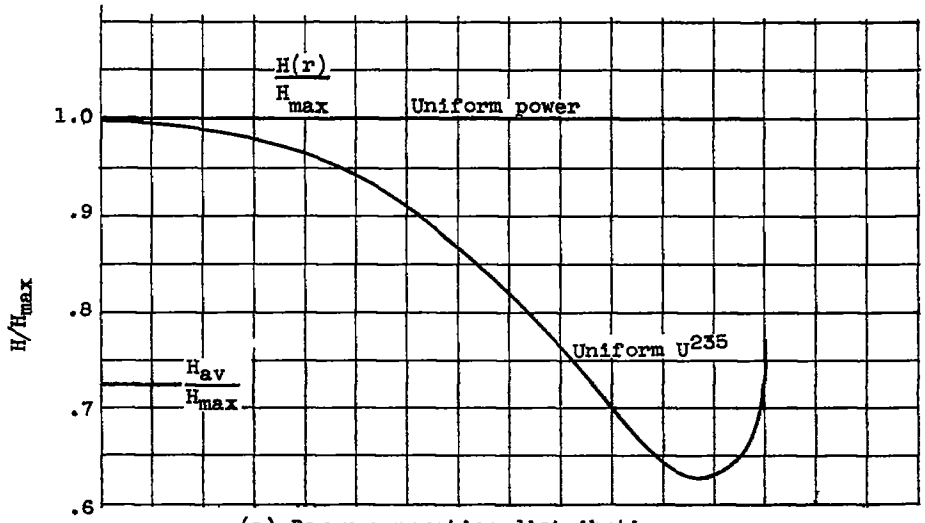

(a) Power generation distribution.

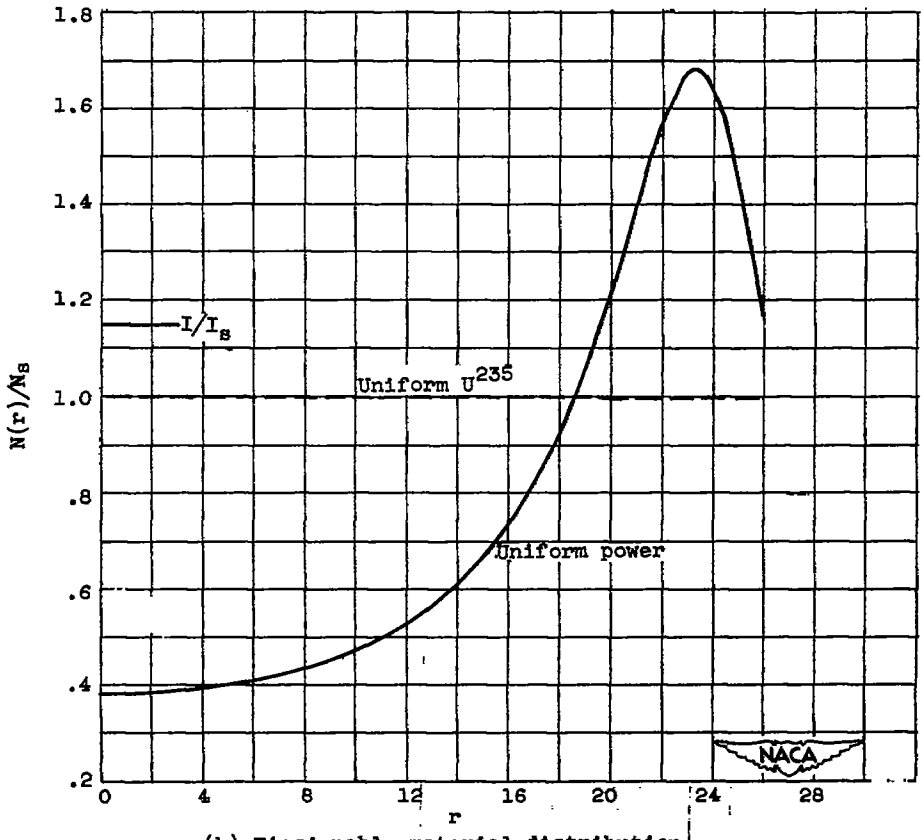

(b) Fissionable material distribution.

Figure 3. - Comparison of power generation and corresponding fissionable material distributions for reactor II, analytical solution. (Relative level of power curves based on a specified limiting heat-flux rate for reactor.)

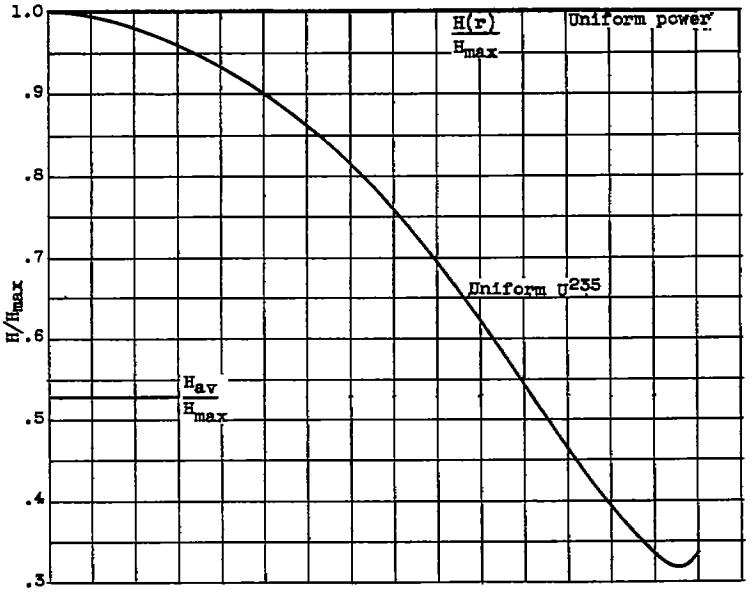

(a) Power generation distribution.

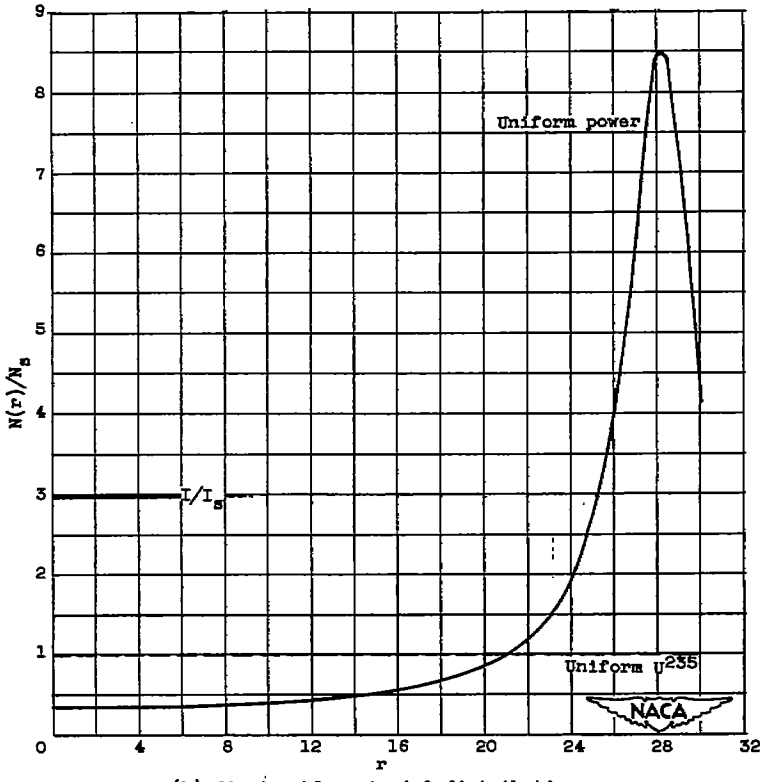

(b) Fissionable material distribution.

Figure 4. - Comparison of power generation and corresponding fissionable material distributions for reactor III, analytical solution. (Relative level of power curves based on a specified limiting heat-flux rate for reactor.)

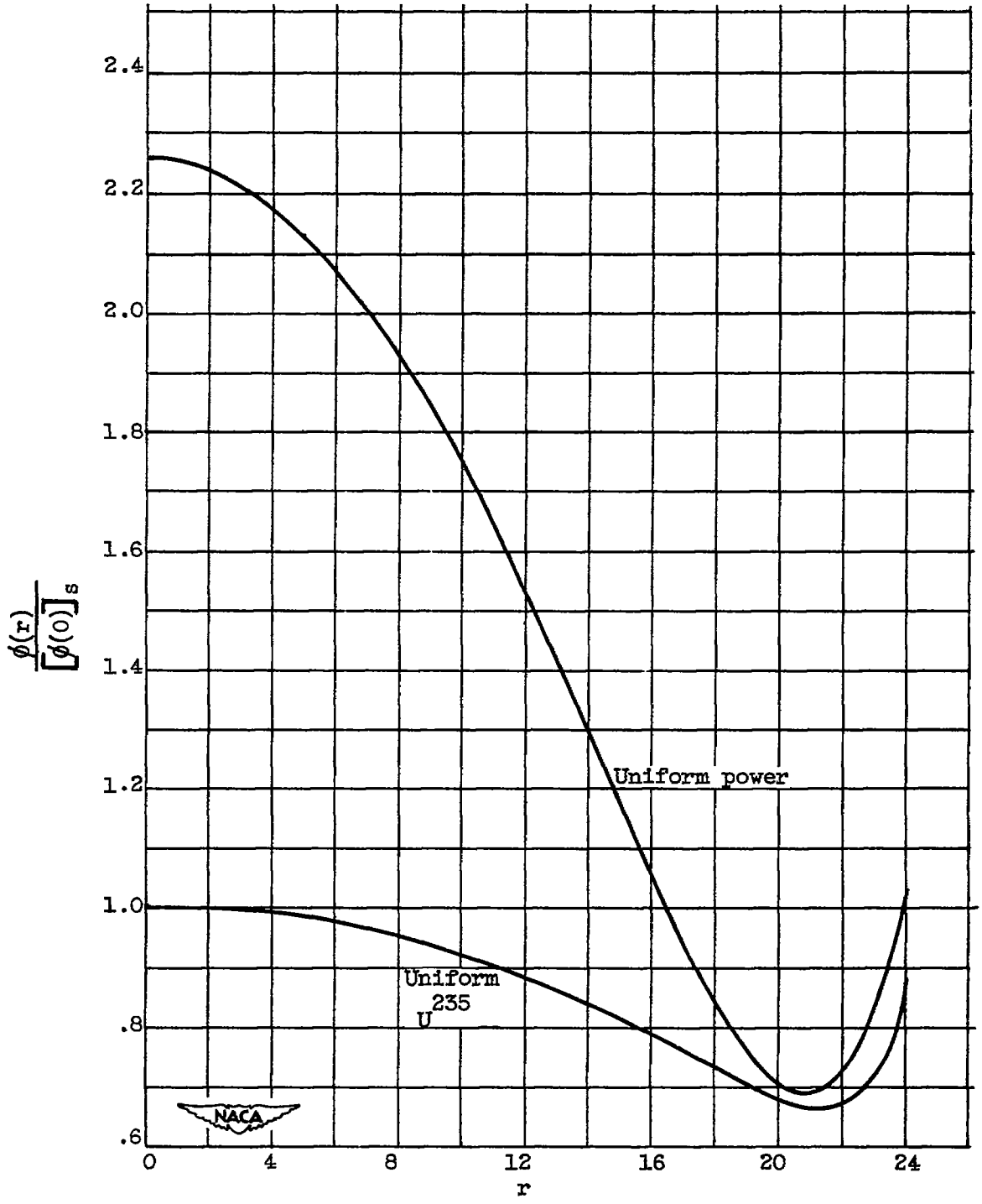

Figure 5. - Comparison of flux distributions for reactor I, analytical solution.

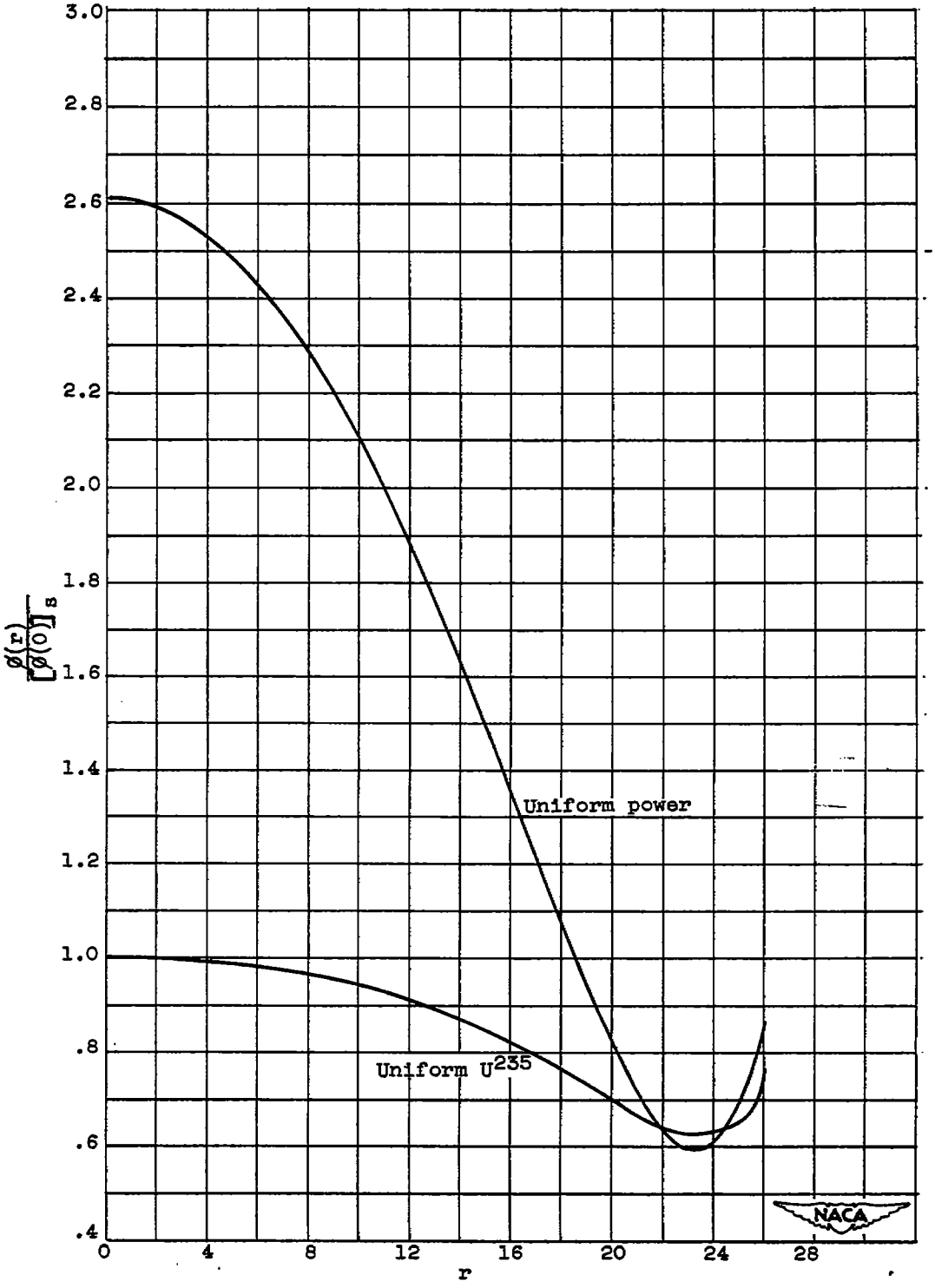

Figure 6. - Comparison of flux distributions for reactor II, analytical solution.

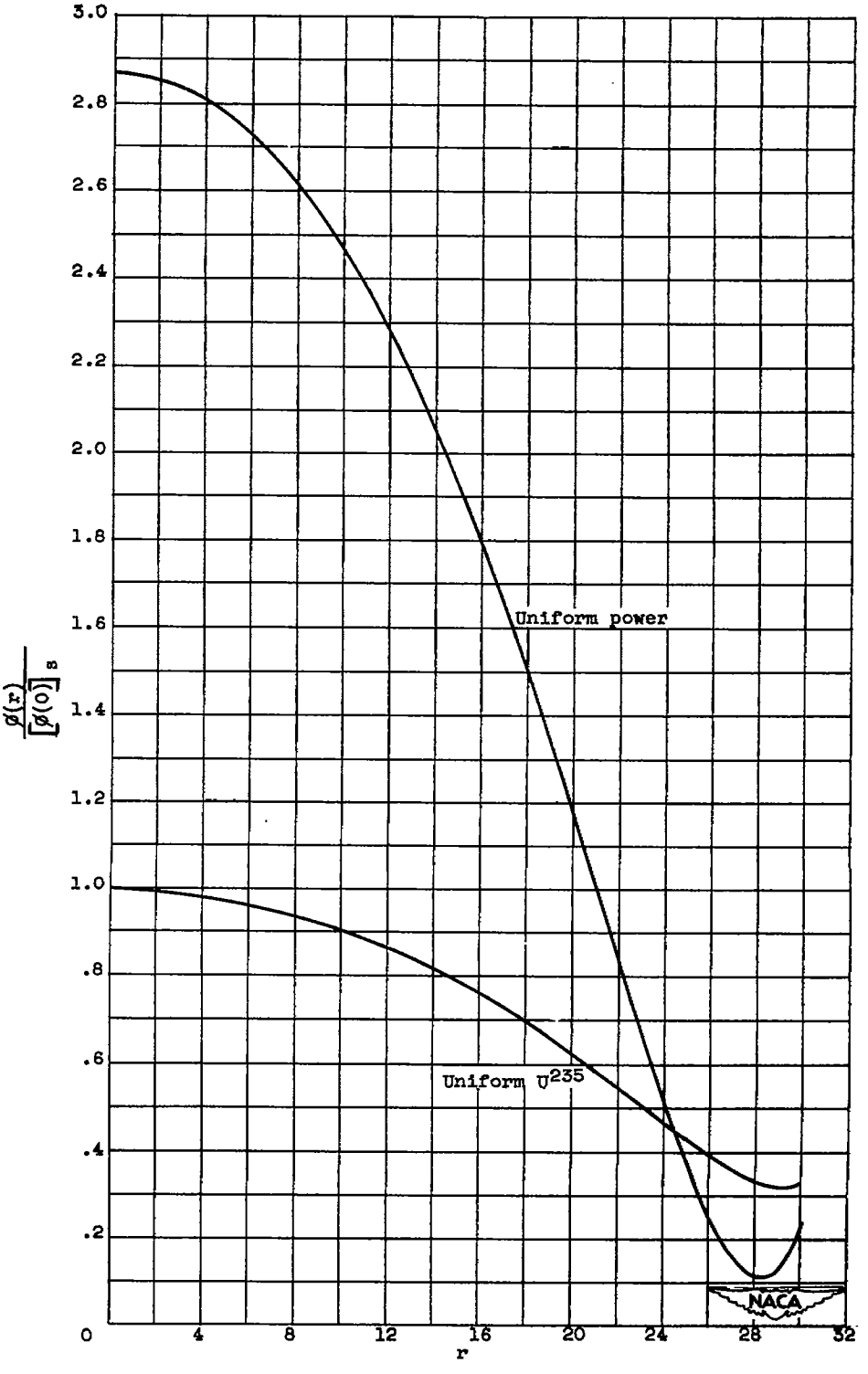

Figure 7. - Comparison of flux distributions for reactor III, analytical solution.

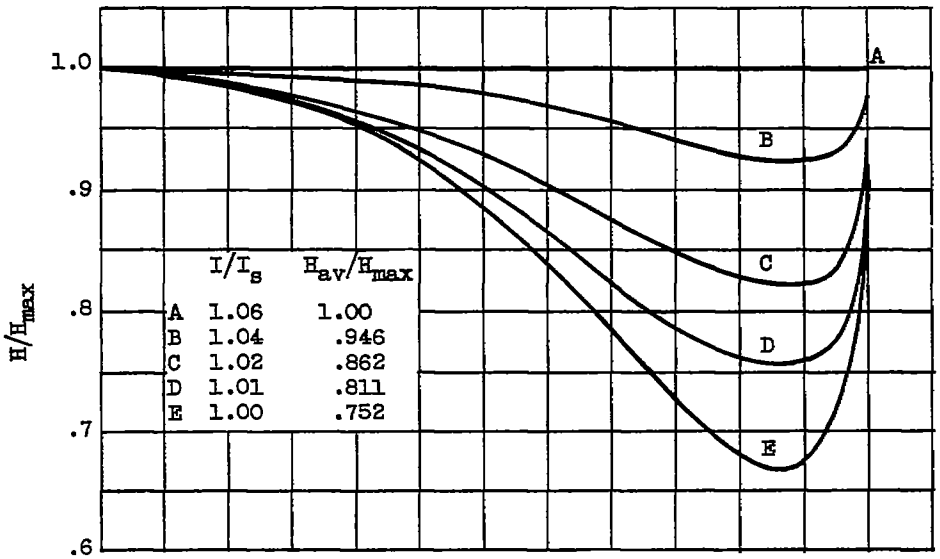

(a) Power generation distribution.

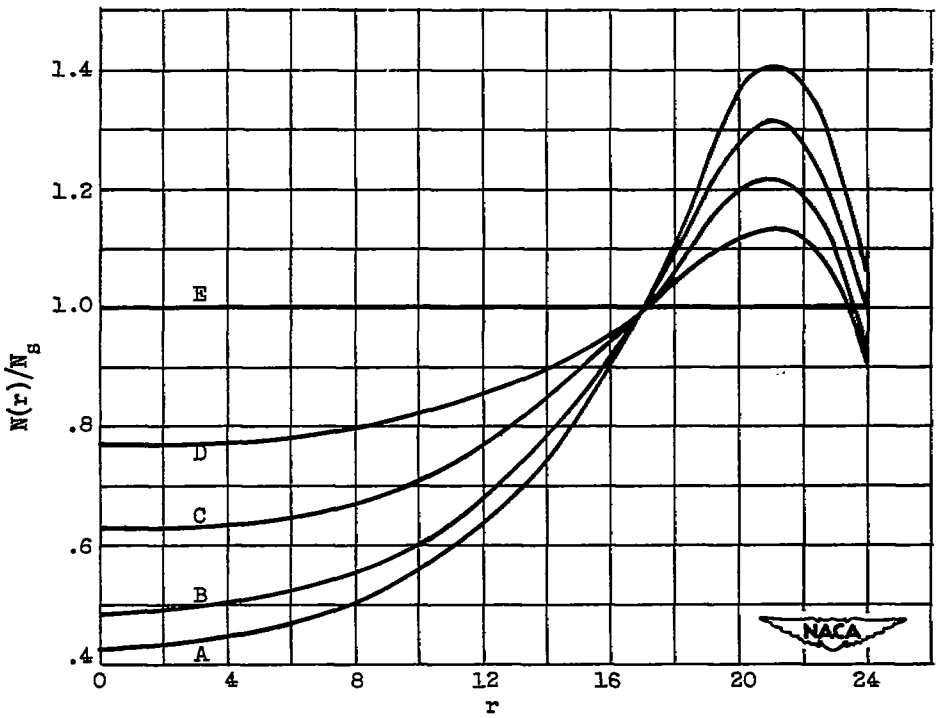

(b) Fissionable material distribution.

Figure 8. - Comparison of power generation and corresponding fissionable material distributions for reactor assembly I, simulator solutions. (Relative levels of power curves based on a specified limiting power density for reactor.)

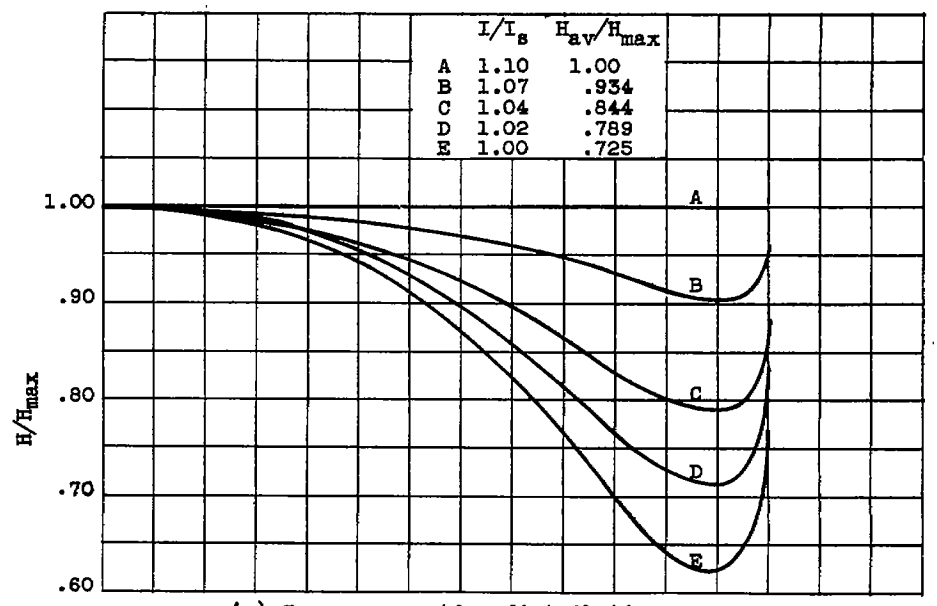

(a) Power generation distribution.

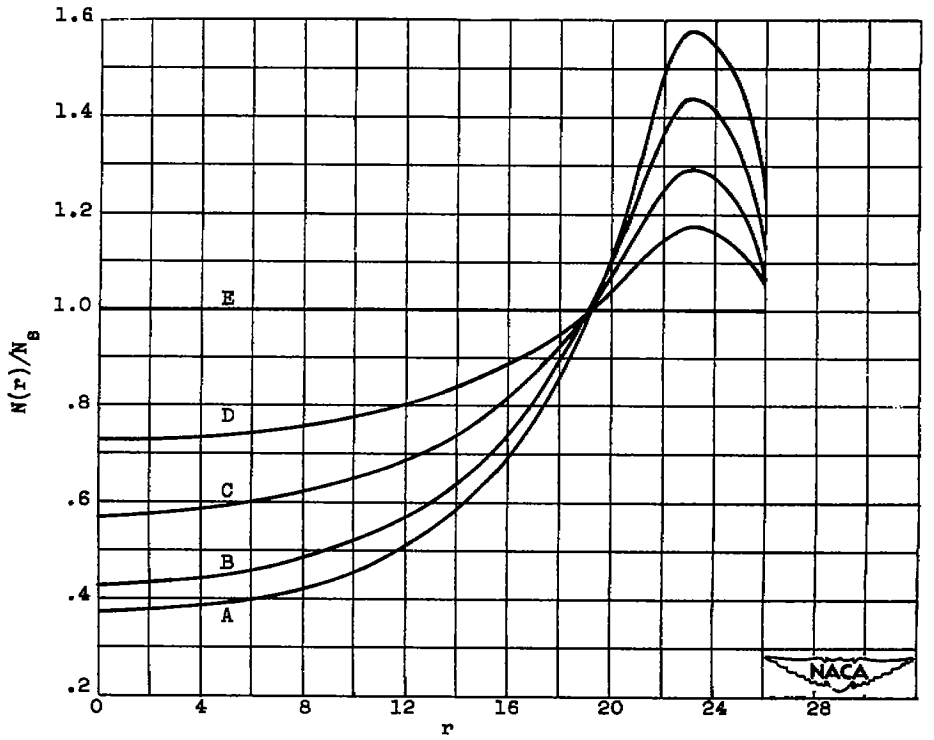

(b) Fissionable material distribution.

Figure 9. - Comparison of power generation and corresponding fissionable material distributions for reactor assembly II, simulator solutions. (Relative levels of power curves based on a specified limiting power density for reactor.)

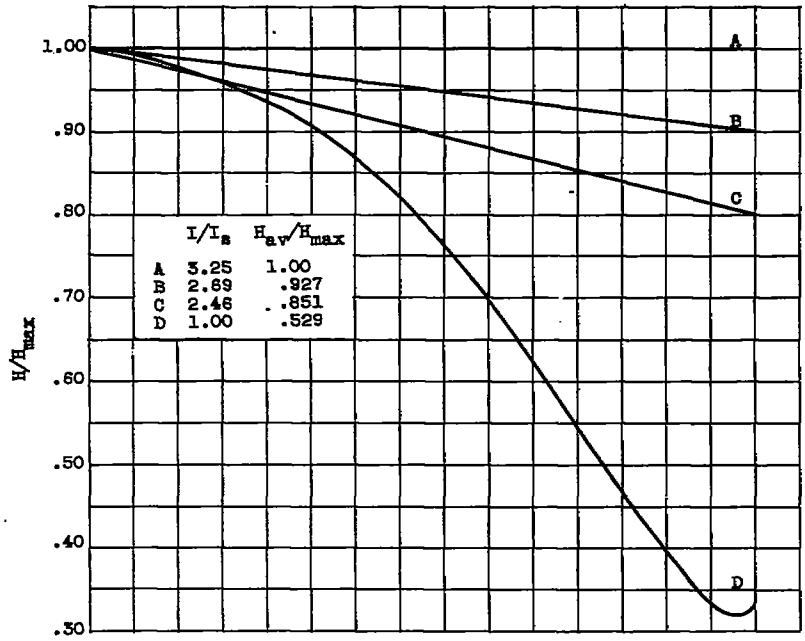

(a) Power generation distribution.

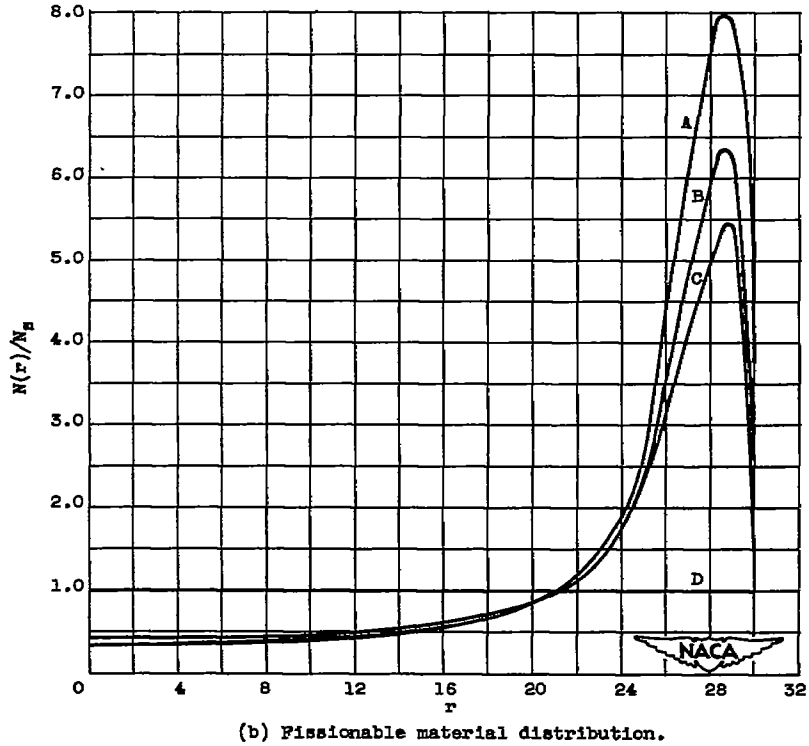

(b) Fissionable material distribution.

Figure 10. - Comparison of power generation and corresponding fissionable material distributions for reactor assembly III, simulator solutions. (Relative levels of power curves based on a specified limiting power density for reactor.)

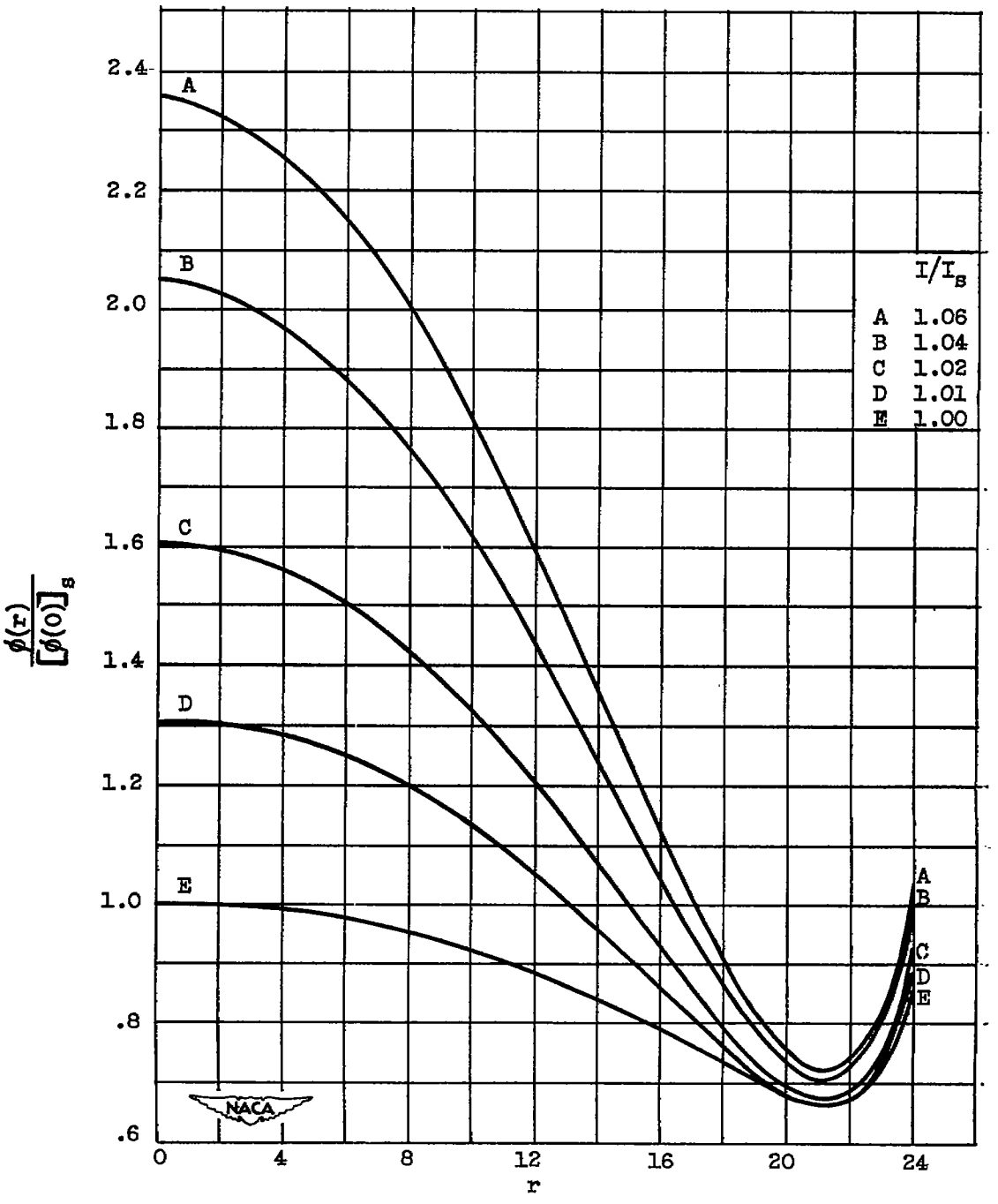

Figure 11. - Comparison of flux distributions for reactor assembly I. (Relative levels of flux curves based on a specified limiting power density for reactor.)

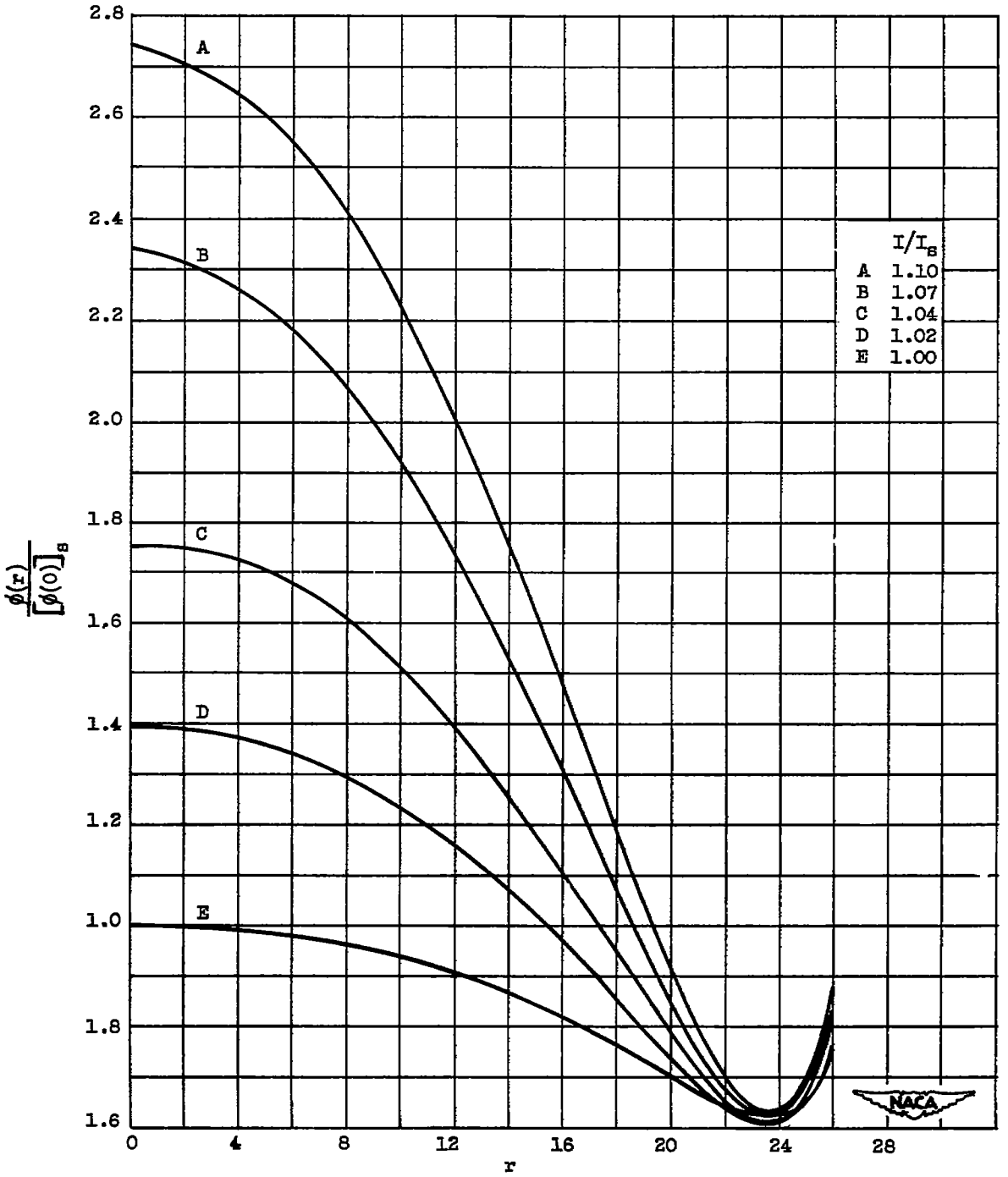

Figure 12. - Comparison of flux distributions for reactor assembly II. (Relative levels of flux curves based on a specified limiting power density for reactor.)

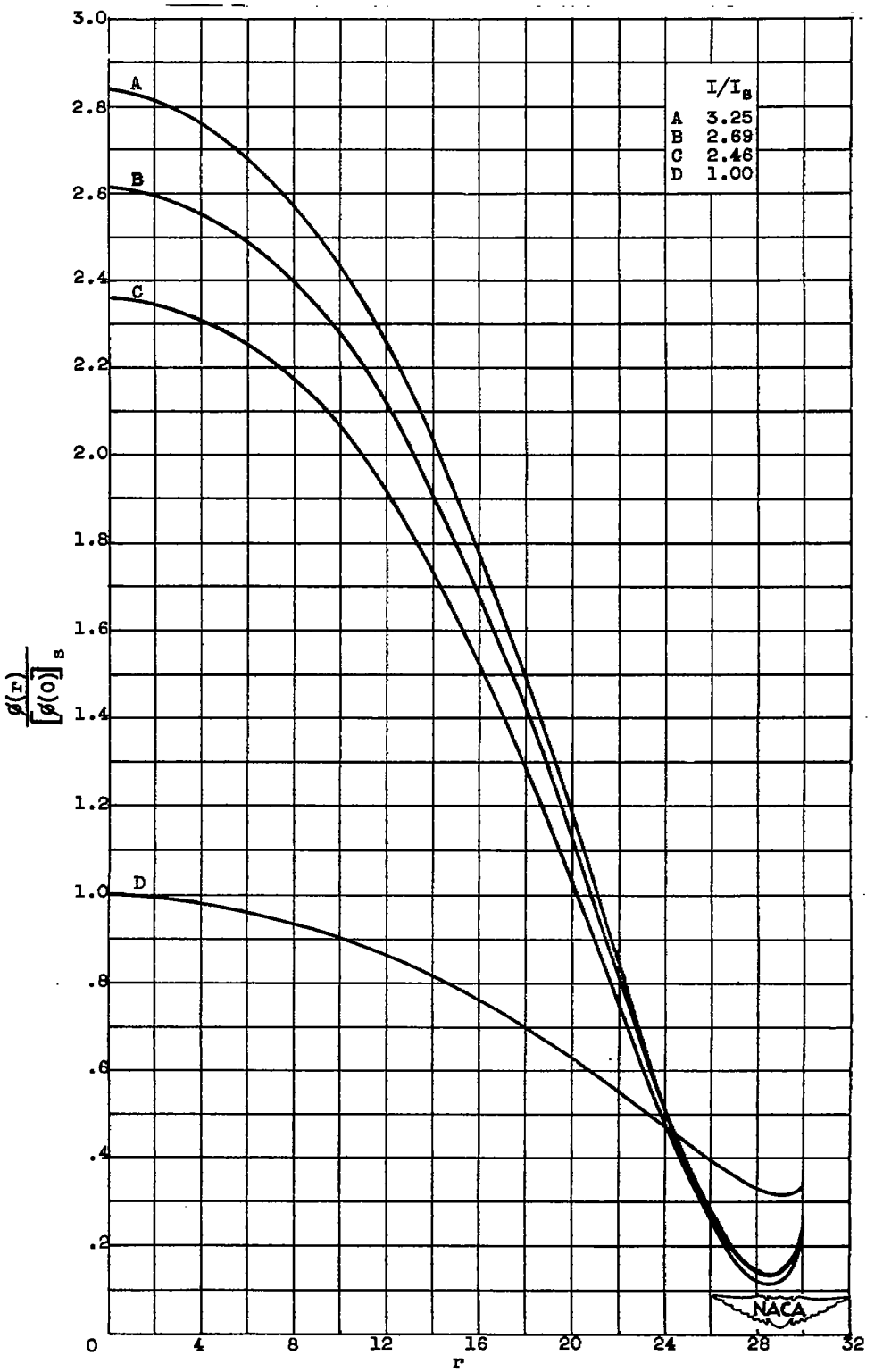

Figure 13. - Comparison of flux distributions for reactor assembly III. (Relative levels of flux curves based on a specified limiting power density for reactor.)